Theoretical Studies of CO Adsorption on Si(100)-2 × 1 Surface

F. T. Bacalzo, D. G. Musaev,* and M. C. Lin*

Department of Chemistry and Cherry L. Emerson Center for Scientific Computation, Emory University, Atlanta, Georgia 30322

Ab initio molecular orbital and density functional calculations have been carried out to investigate the adsorption of CO on the Si(100)-2 × 1 surface using the Si_9H_{12} and $Si_{13}H_{20}$ cluster models of the surface. It was found that B3LYP/6-31G(d) is a reasonable level of theory for calculation of the geometries of the clusters and adsorbates, as well as energetics of the adsorbates of the CO/Si(100)-2 × 1 surface. The addition of a doubly contracted polarizarion d-function for the non-hydrogen atoms changes the calculated CO desorption energy by 1 kcal/mol. Increasing the size of the cluster from Si_9H_{12} to $Si_{13}H_{20}$, in general, increases the CO desorption energy by 1−2 kcal/mol, while it does not change the Si_d-Si_d, Si_d-Si_{sub}, and $Si_{sub}-Si_{sub}$ bond distances, which suggests that the Si_9H_{12} cluster is a good model for the single-dimer cluster. Interaction of the CO molecule with the surface dramatically changes the Si_d-Si_d and Si_d-Si_{sub} bond distances corresponding to the silicon dimer on the surface and that between the first- and second-layer atoms, respectively. These results suggest that the geometry relaxation of the cluster upon interaction with gas molecules should be taken into account. Different adsorption geometries of CO on the silicon surface dimer have been studied. The adsorbed CO is most stable when bonded perpendicularly to the surface dimer with the C atom attached to one of the Si atoms. The calculated CO desorption energy at the B3LYP/6-311G(2d) level, 10.5 kcal/mol, is in good agreement with the experimental value, 11.4 kcal/mol. Vibrational frequencies of the different CO adsorption isomers have been analyzed. For the OC-normal adsorption process, an extensive search for its transition state failed to locate it; this suggests that the adsorption reaction is a nonactivated process with zero barrier.

Introduction

The studies of the mechanism and thermodynamic properties of the gas−surface interaction are extremely important tasks of chemistry. There have been several studies on the weak interaction of CO with Si single-crystal surfaces.[1−10] The first successful measurement for the vibrational spectrum of the adsorbed CO on Si was reported by Bu and Lin[9] with the high-resolution electron energy loss spectroscopy (HREELS) using a Si(100)-2 × 1 surface. Two distinct absorption peaks which appeared at 411.4 and 2081.0 cm^{-1}, corresponding to the Si−CO and SiC≡O stretching vibrations, respectively, were observed. The result of a He I ultraviolet photoelectron spectroscopy (UPS) analysis indicated the intensity of the surface state at 0.8 eV below E_F decreased gradually but slightly with increasing dosage from 0.03 to 4.0 langmuir. The result was attributed to the physical suppression effect of the CO on top of the Si dimers. Temperature-programmed desorption (TPD) measurements using ^{13}CO showed that a single desorption peak appeared at 180 K. Under low dosage (≤0.4 langmuir) conditions, the peak was symmetrical and sharp while for higher dosage (≥1.5 langmuirs) conditions, the peak was broader and asymmetrical. The main feature of our CO/Si(100)-2 × 1 results have been confirmed subsequently by Ho and co-workers,[10] including the effectiveness of UV irradiation on the desorption of the CO.

However, these experimental studies have left unsolved the problems related to the structure of the adsorbed product and the mechanism of the CO/Si(100)-2 × 1 gas−surface interaction. In the present series of studies, we carry out the density

functional and ab initio molecular orbital (MO) calculations to study the interaction of small molecules with the reconstructed Si(100)-2 × 1 surface. Our initial emphasis has been placed on the systems for which we have made extensive surface spectral analyses, for example, CO,[9] HCN,[11] HN$_3$,[12] C$_2$N$_2$,[13] among others. Since this is our first paper in a similar series of studies, we have also examined in detail the effects of the basis set and cluster size, the orientation of the adsorbate, and the methods employed on the calculated adsorption energy and vibrational frequencies. The results are systematically presented herein.

Computational Procedure

In this paper, we have used two types of clusters to simulate the reconstructed Si(100)-2 × 1 surface (see Figure 1). First is a Si_9H_{12} cluster, where the top layer is a dimer consisting of two Si atoms.[14] The second layer contains the four nearest-neighbor atoms of the surface dimer, the third layer with two atoms, and the fourth layer with one neighbor atom. During the surface reconstruction, each surface Si atom forms a σ bond with an adjacent Si atom and leaves two weakly coupled dangling bonds on the incipient dimer, leading to the observed p-(2 × 1) symmetry. To model an extended lattice structure, all dangling bonds of subsurface Si atoms are saturated by H atoms. A single dimer model is used in all our calculations which does not take into account the buckling effect existing in an extended surface. Despite the previous studies[15−17] which indicate that the energy difference between symmetric (unbuckled) and asymmetric (buckled) forms of the Si(100) surface is small, we are planning to do more extensive studies of this effect

TABLE 1: Optimized Bond Lengths (Å) of the Si_9H_{12} and $Si_{13}H_{20}$ Clusters

|		Si_9H_{12}			$Si_{13}H_{20}$	
bond	bulk	B3LYP LANL2DZ	B3LYP 6-31G(d)	MP2 6-31G(d)	B3LYP LANL2DZ	B3LYP 6-31G(d)
Si_d-Si_d	2.45^a	2.213	2.221	2.227	2.225	2.228
Si_d-Si_{sub}	2.35	2.348	2.346	2.329	2.354	2.354
$Si_{sub}-H$		1.485	1.490	1.489	1.489	1.496
$Si_{sub}-Si_{sub}$	2.35	2.383	2.375	2.360	2.390	2.369

[a] Reference 30.
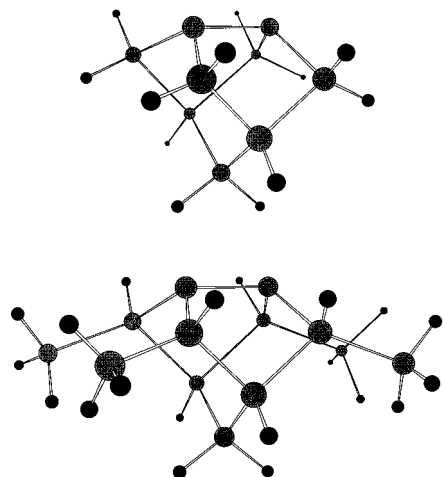
Figure 1. Optimized clusters at the B3LYP/6-31G(d) level.

on our coming paper. Although the Si_9H_{12} cluster is widely used in the literature[14,17–19] as a single-dimer model, the relation of the calculated physical properties and size of the silicon clusters still needs to be reinvestigated; therefore, we have also investigated the $Si_{13}H_{20}$ cluster (see Figure 1), where four Si atoms are added to the second layer of the Si_9H_{12} cluster. These added subsurface Si atoms are saturated with H atoms to terminate all dangling bonds.

In general, the CO molecule may interact with the surface dimer in different ways. In this paper, we study its four different adsorption geometries with the surface dimer (see Figure 2): (1) OC-normal, i.e., CO coordinates to one of the surface Si atoms via its carbon end; (2) CO-parallel, i.e., CO coordinates to the surface dimer in a side-on manner with its CO bond; (3) CO-normal, i.e., CO coordinates to one of the surface Si atoms via its oxygen end; (4) OC-bridge, i.e., CO coordinates to the Si_d-Si_d bond via its carbon end.

Complete geometry optimization (with no constrained degrees of freedom) on all systems in this paper was done using the analytical gradient technique and the hybrid density functional method, B3LYP, including Becke's three-parameter nonlocal-exchange functional[20] with the correlation functional of Lee–Yang–Parr.[21] To elucidate the basis set effect in these calculations, we used several kinds of basis sets. First is the standard LANL2DZ basis set including the D95 double-ζ basis set for the first-row atoms[22] along with Hay and Wadt's effective core potential (ECP) and valence double-ζ basis sets on Si atoms.[23] The ECP employed for Si atoms reduces the number of electrons treated explicitly on each silicon atom from 14 to 4, leading to a considerable reduction in the computational effort. The second basis set used in this paper is the standard all-electron split-valence basis set 6-31G(d)[24] including the polarization d-function on non-hydrogen atoms. To examine the reliability of the used B3LYP method, we also have optimized the geometry of the Si_9H_{12} cluster at the MP2/6-31G-
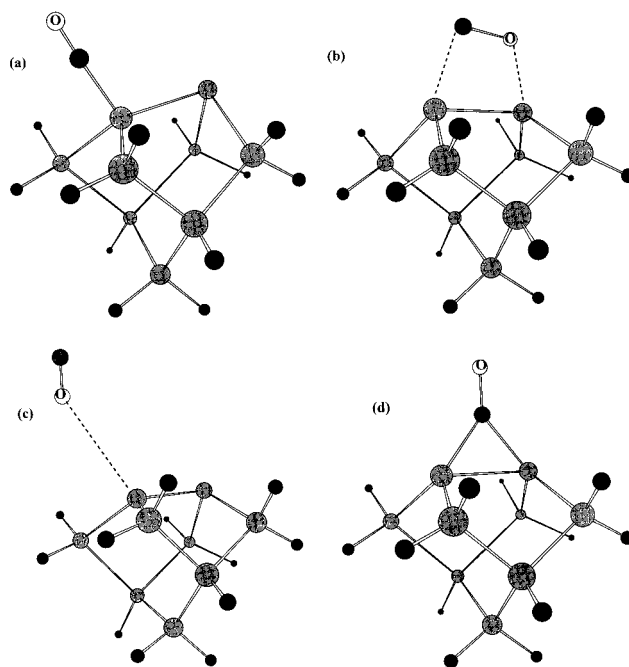
Figure 2. Different Adsorption Geometries of CO. (a) OC-normal, (b) CO-parallel, (c) CO-normal, and (d) OC-bridge. All clusters are optimized at the B3LYP/6-31G(d) level.

(d) level. Due to computational difficulties, the vibrational frequencies were calculated only at the B3LYP/LANL2DZ level.

To further investigate the basis set effect, we have performed more extensive studies on the relative energies of the OC-normal and OC-bridge clusters using the B3LYP method and several kinds of modification for the basis sets, 6-31G and 6-311G,[25] including single and double polarization d-functions for non-hydrogen atoms and a single polarization p_H-function on H atoms (see below for more details).

Final energy parameters include the unscaled zero-point-energy corrections (ZPC) calculated at the B3LYP/LANL2DZ level. All calculations were performed with the GAUSSIAN-94 package.[26]

Results and Discussion

A. Geometries. As mentioned above, a single-dimer cluster model is used to study the adsorption of a CO molecule on the Si(100)-2 × 1 surface. The optimized structure of the Si_9H_{12} and $Si_{13}H_{20}$ clusters are shown in Figure 1, while their important geometrical parameters (Si_d, Si dimer atom; Si_{sub}, subsurface Si atom) are given in Table 1. A close look at Table 1 reveals a maximum 0.01 Å difference in the calculated bond distances obtained at the B3LYP/LANL2DZ and B3LYP/6-31G(d) levels of theory. Note that our results are in close agreement with those obtained by Konecny and Doren[17] using the B3LYP functional and an all-electron valence triple-ζ (TZ94P) basis sets. With regard to the effect of methods used, there is no

CO Adsorption of Si(100)-2 × 1 Surface

J. Phys. Chem. B, Vol. 102, No. 12, 1998 **2223**

TABLE 2: Optimized Bond Distances (Å) at B3LYP Level of the OC-Normal and OC-Bridge Configurations Using Two Cluster Models and Two Basis Sets

	OC-normal				OC-bridge			
	Si_9H_{12}		$Si_{13}H_{20}$		Si_9H_{12}		$Si_{13}H_{20}$	
bond	LANL2DZ	6-31G(d)	LANL2DZ	6-31G(d)	LANL2DZ	6-31G(d)	LANL2DZ	6-31G(d)
C$-$O	1.171	1.144	1.172	1.144	1.225	1.194	1.225	1.192
$Si_d$$-$C	1.838	1.884	1.838	1.886	1.952	1.974	1.959	1.983
$Si_d$$-$$Si_d$	2.535	2.427	2.585	2.454	2.428	2.422	2.432	2.415
$Si_d$$-$$Si_{sub}$	2.392	2.384	2.420	2.405	2.357	2.358	2.361	2.365
$Si_{sub}$$-$$Si_{sub}$	2.360	2.361	2.360	2.365	2.364	2.367	2.370	2.365
$Si_{sub}$$-$H	1.485	1.491	1.487	1.492	1.484	1.492	1.486	1.491

TABLE 3: Total and Dissociation Energies $D_e = E_{CO} + E_{Si(100)} - E_{CO/Si(100)}$

	D_e (kcal/mol)			
	OC-normal		OC-bridge	
method/basis set	Si_9H_{12}	$Si_{13}H_{20}$	Si_9H_{12}	$Si_{13}H_{20}$
B3LYP/LANL2DZ	12.88 (11.56)[a]	13.05	15.32 (13.46)[a]	16.47
B3LYP/6-31G(d)	12.20 (10.88)	11.57	4.08 (2.22)	5.83
MP2/6-31G(d)[b]	4.20 (2.88)	5.44	−4.64 (−6.50)	−1.95
experiment	11.4[c]			

	total energy (au)			
	OC-normal		OC-bridge	
method/basis set	Si_9H_{12}	$Si_{13}H_{20}$	Si_9H_{12}	$Si_{13}H_{20}$
B3LYP/LANL2DZ	−155.413 349	−175.749 566	−155.417 238	−175.755 024
B3LYP/6-31G(d)	−2725.994 819	−3888.798 648	−2725.981 871	−3888.789 500
MP2/6-31G(d)[b]	−2720.974 684	−3881.639 160	−2720.960 594	−3881.627 374

[a] Quantities in parentheses are dissociation energies calculated with zero-point energy correction at the B3LYP/LANL2DZ level. [b] MP2/6-31G(d) single-point calculations using the B3LYP/6-31G(d) geometries. [c] Reference 28.

considerable change in the geometric parameters of the Si_9H_{12} cluster obtained at the MP2/6-31G(d) and B3LYP/6-31G(d) levels. Since the B3LYP/6-31G(d) is much cheaper than the MP2/6-31G(d) and provides almost the same results as the MP2/6-31G(d) with respect to geometries, we will use the B3LYP/6-31G(d) method for optimization of geometries of our cluster model.

As seen in Table 2, where we have shown the optimized geometries of the different possible structures (see also Figure 2, discussion given below) of the adsorbed CO/Si_9H_{12} and CO/$Si_{13}H_{20}$ systems, the bond distances of the adsorbed state at the B3LYP/LANL2DZ and B3LYP/6-31G(d) levels of theory are very different, especially the Si_d−C and Si_d−Si_d bond distances for the OC-normal isomer where it can be as much as 0.10 Å. Therefore, below we will only discuss the geometry parameters calculated at the B3LYP/6-31G(d) level. The optimization of the geometries of the adsorbed CO/Si_9H_{12} and CO/$Si_{13}H_{20}$ systems at the MP2/6-31G(d) level was technically impossible within our computational facilities. We believe that the B3LYP/6-31G(d) method is reliable in describing the geometries of the adsorbed CO/Si_9H_{12} and CO/$Si_{13}H_{20}$ systems.

In an effort to investigate the effect of cluster size of the single dimer model on the geometrical parameters, we have considered the $Si_{12}H_{20}$ model introduced by Jing and Whitten.[15] Complete optimization of the cluster without any symmetry constraints resulted in a flattened cluster, hence not simulating the correct Si(100)-2 × 1 surface. We, therefore, added a fourth layer with a single Si atom and terminated its dangling bonds with two hydrogen atoms. As seen in Tables 1 and 2, the geometries of the resulting $Si_{13}H_{20}$ cluster, as well as the adsorbed CO/$Si_{13}H_{20}$ systems optimized with no symmetry constraints, are very close with the small cluster Si_9H_{12} and adsorbed CO/Si_9H_{12} systems, respectively. *In other words, increasing the size of the cluster modeling single-dimer surface Si(100) does not change the geometric parameters, especially*

the surface Si dimer distance. This suggests that, in terms of the geometry, the Si_9H_{12} cluster is a good model for the single-dimer clusters.

Comparison of the B3LYP/6-31G(d) data presented in Tables 1 and 2 shows that coordination of the CO molecule to the Si clusters changes the geometries of the latter. The Si_d−Si_d bond distance corresponding to the silicon dimer on the surface elongates by 0.20−0.23 Å. The next large difference, 0.04−0.05 Å, occurs in the Si_d−Si_{sub} distance which corresponds to the distance between the first- and second-layer silicon atoms. The changes in the Si_{sub}−Si_{sub} distance corresponding to the second- and third-layer silicon atoms are negligible. These results demonstrate that the geometry relaxation of the cluster upon interaction with gas molecules is significant and should be taken into account.

B. Adsorbate Configurations and Desorption Energies. Figure 2 shows the different isomers of CO adsorption on the Si surface that are studied in this paper. Vibrational analyses performed at the B3LYP/LANL2DZ level suggest that all of these isomers are real minima with no imaginary frequencies. However, we will mainly discuss the isomers OC-normal and OC-bridge because the isomers CO-parallel and CO-normal lie about 20−30 kcal/mol higher than the OC-normal and are metastable to dissociation of the CO molecule.

Table 3 shows the calculated total and desorption energies calculated at the different levels of theory and for the clusters Si_9H_{12} and $Si_{13}H_{20}$. The calculated desorption energies of the OC-normal and OC-bridge are compared with the result of a recent temperature-programmed desorption (TPD) experiment carried out in our laboratory.[26] From this table, we can make several conclusions. First, at the B3LYP/LANL2DZ level, the OC-bridge isomer is a few kcal/mol more stable than the OC-normal isomer. Increasing the basis set from LANL2DZ to the 6-31G(d) changes these isomers in the energy scale and makes the OC-normal isomer about 6−10 kcal/mol more stable than

TABLE 4: Basis Set Effect on the Total Energies and Dissociation Energies of OC-Normal and OC-Bridge Geometries Using B3LYP

	total energy			dissociation energy (kcal/mol)	
basis set	OC-normal (au)	CO molecule + Si_9H_{12} cluster (au)	$\Delta E_t{}^a$ (kcal/mol)	OC-normal	OC-bridge
6-31G(d)	−2725.994 819	−2725.975 368	8.12	12.20	4.08
6-31G(d,p)	−2726.008 133	−2725.988 366	8.24	12.40	4.16
6-31G(2d)	−2726.014 276	−2725.992 559	10.56	13.63	3.07
6-311G(d)	−2726.222 324	−2726.207 548	8.77	9.27	0.50
6-311G(d,p)	−2726.241 567	−2726.226 817	8.67	9.26	0.58
6-311G(2d)	−2726.239 155	−2726.222 431	10.15	10.49	0.35

^{a} ΔE_t is the difference between the OC-normal and OC-bridge total energies.

the OC-bridge isomer, which qualitatively agrees with the MP2/ 6-31G(d)//B3LYP/6-31G(d) results. In other words, the small LANL2DZ basis set is not sufficient to describe the energetics of the CO/Si(100) surface interaction and will be ignored hereon. Second, increasing the cluster size increases the CO desorption energy by 1−2 kcal/mol with the exception of the OC-normal isomer calculated at the B3LYP/6-31G(d) level. Third, the calculated desorption energies decrease via B3LYP/6-31G(d) > MP2/6-31G(d)//B3LYP/6-31G(d), which may be attributed to the existence of a small HOMO−LUMO gap in the clusters. The nature of the Si_{3p} orbitals and the orientation of the dangling orbitals lead to weak π-like bonds in the surface dimer of the clusters. The weak coupling of the dangling bonds gives rise to a small HOMO−LUMO gap; i.e., there exists a low-lying triplet state and a singlet state.[18] Nachtigall and co-workers,[19] in their QCISD(T) calculations of the Si_9H_{12} cluster, have identified the singlet state lower in energy than the triplet state by only a few kcal/mol. Since the perturbation theory takes into account the energy difference between the HOMO and LUMO orbitals, the B3LYP method is more suitable in describing the system.[27] Thus, the B3LYP/6-31G(d) method describes the CO/Si(100)-2 × 1 surface much better than the B3LYP/LANL2DZ and the MP2/6-31G(d)//B3LYP/6-31G(d) methods. Finally, the OC-normal desorption energy, 12.20 and 11.57 kcal/mol for the clusters Si_9H_{12} and $Si_{13}H_{20}$, respectively, agrees well with experiment which at the lowest coverage feasible (0.01 langmuir) is found to be 11.4 kcal/mol.[28]

To further investigate the basis set effect, we have performed additional and even more extensive studies on the OC-normal and OC-bridge clusters using the B3LYP method. We utilized two groups of basis sets, 6-31G(d) and 6-311G(d), each group with (1) an additional single polarization p_H-function on H atoms, i.e., (d,p), and (2) an extra set of d-function, i.e., two polarization d-function on Si, C, and O atoms (2d). Table 4 shows the summary of our single-point calculations at the B3LYP/6-31G(d) optimized geometries of OC-normal and OC-bridge. The results are indicative of the following: First, the additional p-type function is not important as the changes in relative energies ΔE_t and binding energies are within 0.2 kcal/ mol, e.g., between 6-31G(d) and 6-31G(d,p), and 6-311G(d) and 6-311G(d,p), respectively. However, the addition of a second d-function has the most effect as the change in both the relative energies and binding energies is at least 1 kcal/mol. Second, although the relative energies ΔE_t did not vary significantly by changing the basis sets from 6-31G(d), 6-31G-(d,p), and 6-31G(2d) to 6-311G(d), 6-311G(d,p), and 6-311G-(2d), respectively, the binding energies reduced by about 3 kcal/ mol. It is worth noting that the 6-311G(2d) basis set gives the best result compared with the experimental desorption energy of 11.4 kcal/mol. Finally, in all the calculations, the OC-bridge isomer has lower binding eneries, confirming that the OC-normal structure is more stable than the OC-bridge one.

To determine the reaction barrier for the CO adsorption process, we have also carried out an extensive search for the existence of transition state (TS) by varying the OC−Si distance of the most stable OC-normal isomer from 1.9 to 2.3 Å. The system energy was found to increase gradually from the adsorbed state to that of the dissociated state, CO + Si(100)-2 × 1, without a well-defined TS. Accordingly, the activation energy for the adsorption reaction is negligibly small, and the reaction is not thermally activated.

After the submission of our paper, a study made by Hu et al.[29] came to our attention. They observed a nonthermally accessible phase for CO on the Si(100) surface using an energetic molecular beam of CO. They found that thermal CO led to the T-CO phase (i.e., the OC-normal structure in our case) and translationally energetic CO which leads to a new phase BT-CO, a combination of T-CO and bridge bound B-CO (which is the OC-bridge isomer in this paper). From the electron energy loss spectra of CO adsorbed on Si(100), they have identified the 2105.16 and 1701.87 cm^{-1} peaks as the T-CO and B-CO, respectively. Further, the temperature-programmed desorption spectra showed desorption energies of 11.5 and 12.7 kcal/mol for T-CO and B-CO, respectively. Hu and co-workers[29] also characterized the BT-CO phase by first principles quantum mechanical methods. To model the Si(100)-2 × 1 surface, they used the Si_9H_{12} cluster. They carried out DFT calculations using the Becke−Perdew−Zunger method and the Bachelet−Hamann−Schlüter pseudopotential (see original paper for more detail). The 6-31G(d,p) Gaussian basis set was used. Their calculated results are as follows: binding energies of 14.53 and 8.30 kcal/mol, C−O bond distances of 1.144 and 1.191 Å, and Si_d−Si_d bond distances of 2.394 and 2.401 Å for T-CO and B−CO, respectively. Comparison of Hu and co-workers[29] results with those given in the present paper shows that (1) our calculated adsorption energy, 10.49 kcal/mol, at the B3LYP/ 6-311G(2d) level agrees very well with their experimental value, 11.53 kcal/mol, while it is about 4 kcal/mol smaller than their calculated value. Second, our and their calculations indicate that the B-CO phase (the OC-bridge isomer in our case) is higher in energy than the T-CO phase (the CO-normal isomer in this paper) by a few kcal/mol. Third, their calculated geometrical parameters have a maximum difference of 0.04 Å from the corresponding values presented in our paper.

Thus, the results presented in this paper are, in general, in excellent agreement with those obtained independently by Hu and co-workers[29] based on the Si_9H_{12} cluster model using a similar density functional theory approach.

C. Vibrational Frequencies. In Table 5 we have compared the calculated vibrational frequencies for the OC-normal and OC-bridge isomers with experiment[9] including the free CO molecule. The calculated frequencies for the OC-normal geometry are in good agreement with the experiment.[9] Moreover, the CO stretching mode at 1993.02 cm^{-1} is slightly red-

CO Adsorption of Si(100)-2 × 1 Surface

J. Phys. Chem. B, Vol. 102, No. 12, 1998 **2225**

TABLE 5: Vibrational Frequencies (cm^{-1}) of CO Adsorbed on Si(100) Surface Calculated at the B3LYP/LANL2DZ Level

mode	expt[a]	OC-normal	% dev	OC-bridge	% dev	free CO
ν_{Si-CO}	411.34	459.85	10.55	562.29	26.84	
ν_{SiC-O}	2080.91	1993.02	4.41	1693.54	22.87	2145.48[b]

[a] Reference 9. [b] ν_{C-O} of free CO molecule.

shifted from its free molecular value of 2145.48 cm^{-1}. This suggests a weak interaction between CO and the cluster for the OC-normal geometry, and thus, a low Si−CO stretching mode is expected. The small red shift in the CO stretching mode is mainly due to the poor electron back-donation from the surface Si atom to the CO molecule. On the other hand, for the OC-bridge geometry, the Si−CO and SiC−O stretching frequencies are 562.29 and 1693.54 cm^{-1}, respectively. The relatively large red shift of the CO stretching mode could be attributed to the existence of the two bonds between the C atom and the surface Si dimer. Furthermore, the effect of anharmonicity is not included in the calculations which may have given rise to the large deviation of the calculated frequencies from experiment. However, the inclusion of such scaling for the anharmonicity would lower the SiC−O vibrational frequency even more.

Conclusion

From the present research, the following conclusions can be drawn:

The B3LYP/6-31G(d) approximation is a reasonable level of theory for calculation of the geometries of the clusters and adsorbates of the adsorbates CO on the Si(100)-2 × 1 surface. The addition of polarization p$_H$-function is not important, whereas the effect on the relative energies is significant from the addition of a second polarization d-function. The binding energies were reduced by about 3 kcal/mol upon going from 6-31G-type basis sets to 6-311G-type ones. The B3LYP/6-311G(2d) method gives the best result compared with our experimental desorption energy of 11.4 kcal/mol,[9] which is in close agreement with the value of Hu et al., ~11.5 kcal/mol.[28]

Increasing the size of the cluster from Si$_9$H$_{12}$ to Si$_{13}$H$_{20}$, in general, increases the CO desorption energy by 1−2 kcal/mol while it does not change the geometrical parameters Si$_d$−Si$_d$, Si$_d$−Si$_{sub}$, and Si$_{sub}$−Si$_{sub}$ bond distances. This suggests that, in terms of the geometry and energetics, the Si$_9$H$_{12}$ cluster is a good model for describing the single-dimer clusters.

Upon interaction with the CO molecule, the geometries of the clusters change dramatically, especially the bond distances Si$_d$−Si$_d$ and Si$_d$−Si$_{sub}$ corresponding to the silicon dimer on the surface and that between the first- and second-layer silicon atoms, respectively. This suggests that the geometry relaxation of the cluster upon interaction with gas molecules should be taken into account. Geometries between the second−third-layer and third−fourth-layer silicon atoms do not change and can be neglected.

Four different adsorbate configurations of CO on the Si surface are found and identified as minima, among which the OC-normal is the global minimum. Isomer OC-bridge is found to be 6−10 kcal/mol higher in energy. The formation of the OC-normal adsorbate was found to occur without a reaction barrier, in accordance with experimental findings.

Results of our vibrational frequency calculations for the OC-normal and OC-bridge configurations show that the interaction between the CO and the Si(100)-2 × 1 surface is weak as revealed by the low Si−CO stretching vibration mode and the small red shift in the CO stretching mode in comparison with that observed in the free CO molecule. The small red shift is attributed to the poor electron back-donation from the surface Si atom to the CO molecule.

References and Notes

(1) Dylla, H. F.; King, J. G.; Cardillo, M. J. *Surf. Sci.* **1978**, *74*, 141.
(2) Burton, L. C. *J. Appl. Phys.* **1972**, *43*, 232.
(3) Joyce, B. A.; Neave, J. H. *Surf. Sci.* **1973**, *34*, 401.
(4) Onsgaard, J.; Heiland, W.; Taglauer, E. *Surf. Sci.* **1980**, *99*, 112.
(5) Sakurai, T.; Hagstrum, H. D. *Phys. Rev. B* **1979**, *20*, 2423.
(6) Lee, F.; Backman, A. L.; Lin, R.; Gow, T. R.; Masel, R. I. *Surf. Sci.* **1989,** *216*, 173.
(7) Forster, A.; Lüth, H. *J. Vac. Sci. Technol. B* **1989**, *7*, 720.
(8) Chamberlain, J. P.; Clemons, J. L.; Gillis, H. P. *Desorption Kinetics of CO from Si(100)-2 × 1.* Presented at the 21st Annual Symposium Applications of Vacuum Science and Technology, Clearwater, FL, Feb 3−5, 1992.
(9) Bu, Y.; Lin, M. C. *Surf. Sci.* **1993**, *298*, 94.
(10) Young, R. W.; Brown, K. A.; Ho, W. *Surf. Sci.* **1995**, *336*, 85.
(11) Bu, Y.; Ma, L.; Lin, M. C. *J. Phys. Chem.* **1993**, *97*, 7081.
(12) Bu, Y.; Chu, J. C. S.; Lin, M. C. *Surf. Sci. Lett.* **1992**, *264*, L151.
(13) Bu, Y.; Ma, L.; Lin, M. C. *J. Phys. Chem.* **1995**, *99*, 1046.
(14) Wu, C. J.; Carter, E. A. *Chem. Phys. Lett.* **1991**, *185*, 172.
(15) Jing, Z.; Whitten, J. L. *Surf. Sci.* **1992**, *274*, 106.
(16) Wiesendanger, R.; Bürgler, D.; Tarrach, G.; Güntherodt, H. J. *Surf. Sci.* **1992**, *274*, 93.
(17) Konecny, R.; Doren, D. J. *J. Chem. Phys.* **1997**, *106*, 2426.
(18) Redondo, A.; Goddard III, W. A. *J. Vac. Sci. Technol.* **1982**, *21*, 344.
(19) Nachtigall, P.; Jordan, K. D.; Sosa, C. *J. Phys. Chem.* **1993**, *97*, 11666.
(20) (a) Becke, A. D. *J. Chem. Phys.* **1993**, *98*, 5648. (b) Becke, A. D. *J. Chem. Phys.* **1992**, *96*, 2155. (c) Becke, A. D. *J. Chem. Phys.* **1992**, *97*, 9173.
(21) Lee, C.; Yang, W.; Parr, R. G. *Phys. Rev. B* **1988**, *37*, 785.
(22) Dunning, Jr., T. H.; Hay, P. J. In *Modern Theoretical Chemistry*; Schaefer, III, H. F., Ed.; Plenum: New York, 1977.
(23) (a) Hay, P. J.; Wadt, W. R. *J. Chem. Phys.* **1985**, *82*, 270. (b) Wadt, W. R.; Hay, P. J. *J. Chem. Phys.* **1985**, *82*, 284. (c) Hay, P. J.; Wadt, W. R. *J. Chem. Phys.* **1985**, *82*, 299.
(24) (a) Hariharan, P. C.; Pople, J. A. *Chem. Phys. Lett.* **1972**, *66*, 217. (b) Francl, M. M.; Pietro, W. J.; Hehre, W. J.; Binkley, J. S.; Gordon, M. S.; DeFrees, D. J.; Pople, J. A. *J. Chem. Phys.* **1982**, *77*, 3654.
(25) (a) McLean, A. D.; Chandler, G. S. *J. Chem. Phys.* **1980**, *72*, 5639. (b) Krishnan, R.; Binkley, J. S.; Seeger, R.; Pople, J. A. *J. Chem. Phys.* **1980**, *72*, 650.
(26) Frisch, M. J.; Trucks, G. W.; Schlegel, H. B.; Gill, P. M. W.; Johnson, B. G.; Robb, M. A.; Cheeseman, J. R.; Keith, T.; Peterson, G. A.; Montgomery, J. A.; Raghavachari, K.; Al-Laham, M. A.; Zakrzewski, V. G.; Ortiz, J. V.; Foresman, J. B.; Peng, C. Y.; Ayala, P. Y.; Chen, W.; Wong, M. W.; Andres, J. L.; Replogle, E. S.; Gomperts, R.; Martin, R. L.; Fox, D. J.; Binkley, J. S.; Defrees, D. J.; Baker, J.; Stewart, J. P.; Head-Gordon, M.; Gonzalez, C.; Pople, J. A. *Gaussian 94*, Revision B.3; Gaussian, Inc.: Pittsburgh, PA, 1995.
(27) (a) Baker, J.; Scheiner, A.; Andzelm, J. *Chem. Phys. Lett.* **1993**, *216*, 380. (b) Laming, G. J.; Handy, N. C.; Amos, R. D. *Mol. Phys.* **1993**, *80*, 1121. (c) Johnson, B. G.; Gill, P. M. W.; Pople, J. A. *J. Chem. Phys.* **1993**, *98*, 5612.
(28) Breslin, J.; Lin, M. C. Unpublished data.
(29) Hu, D.; Ho, W.; Chen, X.; Wang, S.; Goddard III, W. A. *Phys. Rev. Lett.* **1997**, *78*, 1178.
(30) Tong, S. Y.; Maldonado, A. L. *Surf. Sci.* **1973**, *34*, 90.